Metallic Stents: Evaluation of MR Imaging Safety

Frank G. Shellock[1]
Vincent J. Shellock

OBJECTIVE. The objective of our investigation was to evaluate safety during MR imaging (i.e., magnetic field interactions, heating, and artifacts) for metallic stents.

MATERIALS AND METHODS. Different types of metallic stents were tested for magnetic field interactions, heating, and artifacts using a 1.5-T MR system. Magnetic field–related translational attraction and torque were assessed using previously described techniques. Heating was evaluated using an infrared thermometer to record temperatures immediately before and after performing MR imaging using a whole-body–averaged specific absorption rate of 1.3 W/kg. Artifacts were assessed by placing the stents inside a fluid-filled phantom and performing MR imaging using fast spoiled gradient-echo and T1-weighted spin-echo pulse sequences.

RESULTS. For the 10 different stents evaluated, we found no magnetic field interactions, the highest temperature change was ≤+0.3°C, and the artifacts involved signal voids that would not create diagnostic problems as long as the area of interest was not positioned exactly where a particular stent was located.

CONCLUSION. The findings of the safety tests indicated that the 10 different metallic stents would be safe for patients undergoing MR imaging procedures using MR systems with static magnetic fields of 1.5 T or less.

Stents are tubular scaffolding devices, typically made from metal, that can be used to create or maintain an opening in a tubular structure within the body that has narrowed or has become blocked because of injury or disease. Stents have been used to treat conditions that affect the esophagus, bronchus, trachea, bile duct, urethra, ureter, and virtually every blood vessel [1–15].

Possible safety issues exist for a patient with a metallic stent undergoing an MR imaging procedure, including movement or dislodgement of the stent by magnetic field interactions, heating of the stent by RF power deposition, and artifacts associated with the stent that can adversely affect the diagnostic quality of the MR imaging examination [7–18]. In general, metallic stents tend to be safe for patients undergoing MR imaging procedures because the stents are made from nonferromagnetic materials [7–17]. Metallic stents made from weakly ferromagnetic materials are considered to be safe for patients in the MR imaging environment after 6–8 weeks, permitting time for tissue ingrowth and granulation to provide in vivo retention of these devices [7–17].

Because of the growing use of stents, many of which have been developed recently for new clinical applications, there is a need to assess the safety aspects of these metallic implants in the MR imaging environment. Therefore, this investigation was conducted to evaluate magnetic field interactions, heating, and artifacts for 10 different metallic stents designed for a variety of uses.

Materials and Methods

Stents

Ten different metallic stents were assessed for safety during MR imaging procedures (Table 1). These stents were selected for evaluation because they represent different types that have been developed for use in a variety of tubular-shaped anatomic sites such as the coronary artery (e.g., Magic Wallstent [Schneider, Minneapolis, MN]), iliac artery (e.g., Iliac Wallstent Endoprosthesis [Schneider]), bronchus (e.g., Tracheobronchial Wallstent Endoprosthesis [Schneider]), and esophagus (e.g., Wallstent Esophageal II Endoprosthesis [Schneider]). Notably, the aforementioned stents may be used for one or more of the indicated clinical applications. The stents ranged in dimensions as follows: lumen diameter, 3.5–28.0 mm; length, 25.0–130.0 mm; wire diameter, 0.07–0.24 mm; and mass, 0.04–6.194 g (Fig. 1 and Table 1).

Assessment of Magnetic Field Interactions

Tests for magnetic field interactions were performed on three randomly selected "finished" versions

Received January 22, 1999; accepted after revision March 1, 1999.

Supported by Schneider Inc., Minneapolis, MN.

[1]Both authors: Department of Radiology, School of Medicine, University of Southern California, Los Angeles, CA 90036. Address correspondence to F. G. Shellock, 7511 McConnell Ave., Los Angeles, CA 90045.

AJR 1999;173:543–547

0361–803X/99/1733–543

TABLE 1 Metallic Stents Evaluated for Safety During MR Imaging: Results of Tests for Magnetic Field Interactions

Stent Type	Size of Stent (mm)		Diameter of Stent Wire (mm)	Mass of Stent (g)	Wire Material[a]
	Diameter	Length			
Wallstent Endoprosthesis or Magic Wallstent	3.5	25	0.07	0.040	Elgiloy and platinum–nickel alloy
Iliac Wallstent Endoprosthesis	5.0	80	0.09	0.279	Elgiloy and platinum–nickel alloy
Iliac Wallstent Endoprosthesis	6.0	90	0.10	0.335	Elgiloy and tantalum
Iliac Wallstent Endoprosthesis	12.0	90	0.14	1.084	Elgiloy and tantalum
Tracheobronchial Wallstent Endoprosthesis	14.0	80	0.17	0.790	Elgiloy
Tracheobronchial Wallstent Endoprosthesis	24.0	70	0.19	1.353	Elgiloy
Wallstent Esophageal II Endoprosthesis	20.0–28.0	130	0.24	4.431	Elgiloy and permalume[b]
Wallstent Endoprosthesis with permalume covering	8.0	80	0.11	0.433	Elgiloy, tantalum, and permalume[b]
Corita Endoluminal Graft for abdominal aoritc aneurysm	27.0	120	0.24	6.194	Elgiloy and corethane[b]
Iliac Wallgraft Endoprosthesis	12.0	90	0.15	1.152	Elgiloy and tantalum

Note.—All stents had a deflection angle of 0° and no torque; all stents were manufactured by Schneider, Minneapolis, MN.

[a] Elgiloy (Elgiloy Specialty Metals, Elgin, IL) is an alloy of cobalt, chromium, nickel, iron, and molybdenum.

[b] Permalume and corethane were used for the covering of the stent.

(i.e., prototypes were not used for this evaluation) of the stents, with the exception of the Corvita Endoluminal Graft (Schneider), of which only one was evaluated. Magnetic field–related translational attraction was assessed for each stent using a previously described procedure known as the deflection angle test [7, 10, 19–22]. This test was conducted using a shielded 1.5-T MR system (General Electric Medical Systems, Milwaukee, WI) [20–22]. Each stent was suspended by a 30-cm-long piece of thread that was attached to the estimated center of the device. The thread was then attached to a plastic protractor so that the angle of deflection from the vertical could be measured. The accuracy of this measuring device is ±0.5°C based on the ability to read the protractor in the MR system [19–22]. The proper alignment of the protractor was maintained in the 1.5-T MR system with the aid of axial, coronal, and sagittal positioning lights.

The deflection angle test was conducted at the position in the shielded 1.5-T MR system where the spatial gradient of the magnetic field was previously determined to be at a maximum (35 cm inside the bore of the MR magnet) to determine the magnetic field attraction with regard to a worst-case condition [19–23]. The highest spatial gradient for this MR system is 450 G/cm. Deflection angles for the stents were measured three times and averaged. The deflection force (F), which was measured in dynes, was calculated with the following formula: $F = mg \times \tan \theta$, where m is the mass of the material; g, the gravitational acceleration (980 cm/sec^2); tan, tangent; and θ, the deflection angle from the vertical in degrees [7, 10, 20–22].

To determine the presence of magnetic field–induced torque, interaction with the static magnetic field was evaluated by placing each stent on a flat, smooth plastic material with intervals of 1 mm etched on the bottom [21, 22, 24]. This procedure was conducted to obtain a qualitative assessment of torque [21, 22, 24]. The stent was placed on the test apparatus perpendicular to the static magnetic field. The test apparatus with the stent was then positioned in the center of the MR system, where the effect of torque force from the 1.5-T static magnetic field is known to be greatest [7, 10, 21, 22, 24]. The stent was directly observed for any type of possible movement with respect to alignment or rotation to the magnetic field. The observation process was facilitated by having one of the investigators inside the bore of the magnet during the test procedure. The test apparatus with the stent was then removed from the bore of the magnet, and the stent was moved 45° relative to its previous position, reinserted into the center of the magnet, and again observed for alignment or rotation. This process was repeated to encompass a full 360° rotation of positions for each stent [21, 22, 24].

Assessment of Heating

A previously described experimental protocol was used to assess MR imaging–related heating of the stents [21, 24–27]. MR imaging was performed using a relatively high level of RF energy with each stent individually positioned in a plastic phantom filled with physiologic saline. For the heating experiments, MR imaging was conducted using a 1.5-T, 64-MHz MR system with the body coil being used to send and receive RF energy. With the intent of depositing an excessive amount of RF energy during MR imaging, a T1-weighted spin-echo sequence was used with the following selected parameters: imaging time, 30 min; axial plane; TR/TE, 134/25; field of view, 48 cm; matrix size, 256 × 128; section thickness, 20 mm; number of excitations, 54; number of echoes, four; phasing direction, anteroposterior; and transmitter gain, 200 [24, 25]. The whole-body–averaged specific absorption rate was 1.3 W/kg, which is a level of exposure to RF energy exceeding that which is typically used for MR imaging in the clinical setting.

A plastic phantom (length, 55 cm; width, 39 cm; height, 25 cm) was filled with 45 l of physiologic saline solution to provide a highly conductive medium to surround the stent and to "load" the MR system [24]. An acrylic frame (length, 50 cm; width, 1 cm; height, 20 cm) was used to position each stent parallel in the phantom, which was then parallel to the bore of the magnet of the MR system. The stent was fixed to

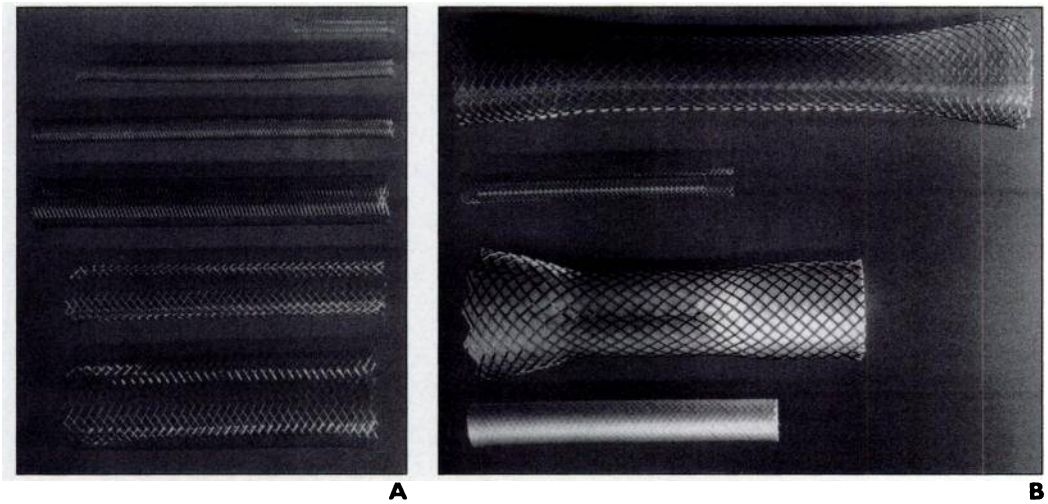

Fig. 1.—Photographs of metallic stents evaluated for safety during MR imaging. All stents were manufactured by Schneider, Minneapolis, MN.
A, Names of stents shown in photograph from top to bottom: Wallstent Endoprosthesis (or Magic Wallstent), Iliac Wallstent Endoprosthesis, Iliac Wallstent Endoprosthesis, Iliac Wallstent Endoprosthesis, Tracheobronchial Wallstent Endoprosthesis, and Tracheobronchial Wallstent Endoprosthesis.
B, Names of stents shown in photograph from top to bottom: Wallstent Esophageal II Endoprosthesis, Wallstent Endoprosthesis with permalume covering, Corvita Endoluminal Graft, and Iliac Wallgraft Endoprosthesis.

the acrylic frame using small strips of porous adhesive tape (Micropore tape; 3M, Minneapolis, MN). The acrylic frame allowed the stent to be immersed in the physiologic saline and to be placed close to the inside of the fluid-filled phantom (within 3 inches [7.6 cm] from the edge), thus permitting the stent to be placed close (within 4 inches [10.2 cm]) to the bore of the magnet. This position (i.e., at the periphery as opposed to the center of the MR system) is the one that is known to have the greater RF heating effect during MR imaging [24]. Because this testing apparatus does not include blood flow, this test further represents an extreme condition for RF heating [24, 25].

A noncontact, infrared thermometer (Medi-Therm; Everest Interscience, Tustin, CA) was used to scan the surface temperatures of each stent [20, 21, 25–27]. This infrared thermometer has an accuracy and resolution of +0.1°C. The infrared thermometer was set to measure a spot of 2.0 mm in diameter; each stent was scanned (i.e., using the Medi-Therm to move over the entire stent to determine the temperatures at multiple positions, including at what might be considered "sharp" points) to determine the highest surface temperature [20, 21, 26, 27]. The highest surface temperature of each stent was determined immediately before and within 5–10 sec after the completion of MR imaging [20, 21, 26, 27]. Because the infrared thermometer is used to assess the surface temperatures of the stents and the measurements are obtained immediately before and after exposure to excessive RF energy (i.e., the surface of the device is scanned, as previously described), this method is capable of evaluating temperature changes in a precise and sensitive manner. This technique of heating assessment for implants exposed to excessive RF energy during MR imaging has been previously reported [20, 21, 26, 27].

The room temperature and the temperature of the bore of the MR system were 21.5°C and 22.0°C, respectively. The fan of the MR system was not on during MR imaging. After obtaining baseline surface temperatures for the stent, MR imaging was performed for 30 min. Immediately after MR imaging, the surface temperatures of the stent were measured. The highest temperature recorded before MR imaging was compared with that obtained immediately after MR imaging; the change in temperature is discussed in the Results.

Assessment of Artifacts

Artifacts associated with the presence of each type of stent were assessed by performing MR imaging of the stent placed inside a plastic phantom filled with distilled water. MR imaging was conducted using a send–receive head coil and the following imaging pulse sequences: fast spoiled gradient-recalled echo in the steady state pulse sequence (50/4; flip angle, 30°; matrix size, 256 × 128; section thickness, 3 mm; field of view, 14 cm; number of excitations, four; bandwidth, 16 kHz) and T1-weighted spin-echo pulse sequence (300/20; matrix size, 256 × 128; section thickness, 3 mm; field of view, 14 cm; number of excitations, 1.5; bandwidth, 16 kHz).

These pulse sequences are commonly used ones that are clinically applied for MR imaging. In addition, the fast spoiled gradient-recalled echo pulse sequence is a partial–flip angle technique that tends to have a great degree of artifact associated with it when MR imaging is performed on a metallic implant [7–11, 20, 21, 24].

The imaging planes were oriented perpendicular and parallel relative to the maximum short axis and maximum long axis of each stent. The frequency-encoding directions were parallel to the planes of imaging for the pulse sequences that were used. Artifacts that result from other positions of the imaging plane relative to the stent or with regard to the particular orientation of the stent to the main magnetic field of the MR system may be slightly more or less than those observed under the specific experimental conditions used in the previously indicated test for artifact assessment. Nevertheless, the MR imaging technique used to assess artifacts is the same as that used in previously performed studies for other metallic implants [20, 21, 24]. For this reason, this technique was selected to assess the stents in this evaluation because it facilitates comparison with previously evaluated implants.

The software provided with the MR system was used to perform planimetry (accuracy and resolution, ±10%) to obtain a cross-sectional area measurement of the artifact size for each stent with regard to the dimensions for each pulse sequence and for each imaging plane [21, 24]. All imaging display parameters (e.g., window and level settings, magnification) were carefully selected and used in a consistent manner to facilitate valid determinations of artifact sizes.

Results

None of the 10 different metallic stents displayed any magnetic field interactions during exposure to the 1.5-T MR system, as indicated by deflection angles of 0° for all stents (deflection forces were also zero) and the lack of any positional changes when the stents were placed in the center of the MR system (Table 1).

For the assessment of heating associated with MR imaging performed using a relatively high level of RF energy, the highest temperature changes recorded from the surface of the stents ranged from +0.1°C to +0.3°C (Table 2). Table 3 provides a summary of the artifacts for the stents

TABLE 2 Heating of Stents During MR Imaging

Stent Type	ΔT (°C)
Wallstent Endoprosthesis or Magic Wallstent	+0.2
Iliac Wallstent Endoprosthesis	+0.1
Iliac Wallstent Endoprosthesis	+0.1
Iliac Wallstent Endoprosthesis	+0.2
Tracheobronchial Wallstent Endoprosthesis	+0.1
Tracheobronchial Wallstent Endoprosthesis	+0.1
Wallstent Esophageal II Endoprosthesis	+0.3
Wallstent Endoprosthesis with permalume covering	+0.1
Corvita Endoluminal Graft for abdominal aortic aneurysm	+0.2
Iliac Wallgraft Endoprosthesis	+0.2

Note.—All stents were manufactured by Schneider, Minneapolis, MN. ΔT = change in temperature.

TABLE 3 Summary of Measurements of Artifacts Seen During MR Imaging of Metallic Stents

Stent Type	Cross-Sectional Area (mm^2) of Artifacts During MR Imaging			
	Fast Spoiled Gradient-Echo		T1-Weighted Spin-Echo	
	Perpendicular Plane	Parallel Plane	Perpendicular Plane	Parallel Plane
Wallstent Endoprosthesis or Magic Wallstent	65	191	28	140
Iliac Wallstent Endoprosthesis	137	535	80	418
Iliac Wallstent Endoprosthesis	109	661	66	571
Iliac Wallstent Endoprosthesis	266	1294	194	1182
Tracheobronchial Wallstent Endoprosthesis	419	1399	269	1297
Tracheobronchial Wallstent Endoprosthesis	969	2061	784	1910
Wallstent Esophageal II Endoprosthesis	793	3352	755	3119
Wallstent Endoprosthesis with permalume covering	142	818	77	681
Corita Endoluminal Graft for abdominal aoritc aneurysm	1911	3078	1622	2778
Iliac Wallgraft Endoprosthesis	241	1195	131	1172

Note.—All stents were manufactured by Schneider, Minneapolis, MN.

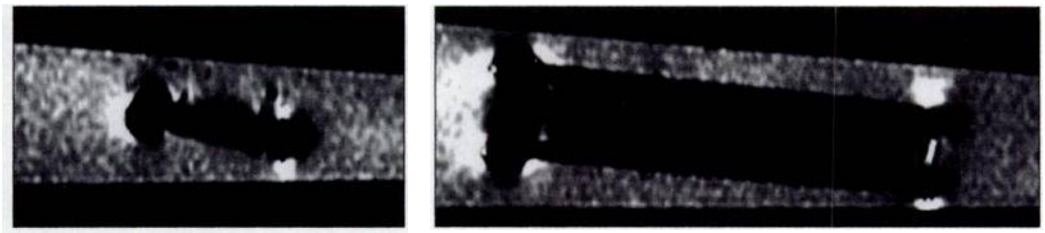

Fig. 2.—Metallic stents (Schneider, Minneapolis, MN) were placed in fluid-filled phantom to assess artifacts. Sagittal MR images were obtained using fast spoiled gradient-echo pulse sequence (TR/TE, 50/4; flip angle, 30°; section thickness, 3 mm; field of view, 14 cm).
A, Wallstent Endoprosthesis (or Magic Wallstent).
B, Tracheobronchial Wallstent Endoprosthesis.

with respect to the cross-sectional area measurements for the two different pulse sequences and imaging planes used for MR imaging. In general, the cross-sectional areas of the artifacts (i.e., the signal voids) were larger for the fast spoiled gradient-recalled echo pulse sequence and smaller for the T1-weighted spin-echo pulse sequence for a given stent. Artifacts for the stents generally showed a signal void relative to the size and shape of the stent as well as to the pulse sequence used for MR imaging (Fig. 2).

Discussion

Magnetic Field Interactions

The two different tests conducted to assess magnetic field interactions (i.e., with respect to translational attraction and torque) for the stents indicated that these devices were unaffected during exposure to the 1.5-T MR system. These findings are consistent with those of other reports in which the lack of magnetic field interactions for metallic implants made from Elgiloy (an alloy of cobalt, chromium, nickel, iron, and molybdenum [Eligiloy Specialty Metals, Elgin, IL]), platinum–nickel alloy, or tantalum is described [7, 8, 10, 16, 17]. Therefore, there would be no risk to a patient undergoing an MR imaging procedure at 1.5 T or less with respect to movement or dislodgement of any of the 10 different metallic stents evaluated in this study.

Heating Effects

There was no substantial heating detected for any stent in association with performing MR imaging using a relatively high level of exposure to RF energy (i.e., the highest temperature change recorded was +0.3°C). The temperature changes were well within physiologically acceptable levels and would not present a hazard to biologic tissues [17, 28, 29]. In general, a metallic implant that has relatively small dimensions or is made from a relatively low mass of metallic material is not considered to present a risk to a patient undergoing an MR imaging procedure [16, 17, 20, 21, 26–30]. Notably, a substantial heat-related injury using MR imaging in a patient with a small metallic implant has never, to our knowledge, been reported [16, 17].

Artifacts

Magnetic susceptibility–related artifacts seen with metallic implants primarily result from disruption of the static and gradient magnetic fields and are directly proportional to the magnetic permeability of the specific materials used to make the devices [7–17, 20, 21, 24]. Eddy currents produced by RF fields during MR imaging may also contribute to the artifacts seen with metallic stents and are primarily dependent on the shape and resistance of the metals that are present [7–10].

Elgiloy is commonly used to make a variety of implants, including aneurysm clips, vena cava filters, and stents [7, 17, 18, 22]. Previous studies have reported that this material produced mild artifacts on MR images compared with other materials used for implants such as 304 and 316L stainless steel, MP35N, and various types of alloys [7, 17, 18, 22, 27]. Likewise, the other materials used to make these stents (i.e., platinum–nickel alloy and tantalum) were reported to produce relatively minor artifacts [7, 9–11, 17, 18, 22, 27].

According to the ex vivo characterization of artifacts for the stents in this study, the fast spoiled gradient-recalled echo pulse sequence produced larger artifacts than the T1-weighted spin-echo pulse sequence. The pulse sequence–dependent effects on artifact size for metallic implants are well-known phenomena and are caused by the particular physical aspects of the pulse sequence technique [7–17, 20, 21]. The relative size of the artifact for a given stent for a given pulse sequence is dependent on a variety of variables including the amount of metal used to make the stent, the magnetic susceptibility of the metals that were used to make the stent, the shape and distribution of the metals, as well as other factors. In general, the artifacts for the stents that were assessed in this study should not greatly affect the diagnostic use of MR imaging, as long as the area of interest is not positioned exactly where the stent is located.

Our evaluation did not assess artifacts for stents that would be present in association with pulse sequences typically used for MR angiography procedures, as has been done in previous studies [9–11, 14]. The primary reason for this omission is that several stents that we evaluated were not intended for intravascular use, and the ex vivo characterization of flow-related artifacts requires technically complicated procedures not within the scope of this study. However, the evaluation of artifacts under flow-related conditions would be of obvious interest for the stents used for endovascular applications, in consideration of the various clinical uses of MR angiography.

In conclusion, ex vivo experiments conducted to assess magnetic field interactions, heating, and artifacts for 10 different stents indicated that MR procedures can be performed safely in patients using MR systems of 1.5 T or less.

References

1. Zollikofer CL, Antonucci F, Markus P, et al. Arterial stent placement with use of the Wallstent: midterm results of clinical experience. *Radiology* **1991**;179:449–456
2. Watkinson AF, Mason RC, Adam A. The role of self-expanding metallic endoprostheses in esophageal strictures. *Semin in Intervent Radiol* **1996**;13:17–26
3. Tesdal IK, Adamus R, Poeckler C, Koepke J, Jaschke W, Georgi M. Therapy for biliary stenoses and occlusions with use of three different metallic stents: single-center experience. *J Vasc Interv Radiol* **1997**;8:869–879
4. Lugmayr H, Pauer W. Self-expanding metal stents for palliative treatment of malignant ureteral obstruction. *AJR* **1992**;159:1091–1094

5. Dyet JF, Shaw JW, Cook AM, et al. The use of the Wallstent in aorto-iliac vascular disease. *Clin Radiol* **1993**;48:227–231
6. Rousseau HP, Dahan M, Lauque D, et al. Self-expandable prostheses in the trachaeobronchial tree. *Radiology* **1993**;188:199–207
7. Teitelbaum CP, Bradley WG Jr, Klein BD. MR imaging artifacts, ferromagnetism, and magnetic torque of intravascular filters, stents, and coils. *Radiology* **1988**;166:657–664
8. Matsumoto AH, Teitelbaum GP, Barth KH, Carvlin MJ, Savin MA, Strecker EP. Tantalum vascular stents: in vivo evaluation with MR imaging. *Radiology* **1989**;170:753–755
9. Teitelbaum G, Ortega HV, Vinitski S, et al. Low-artifact intravascular devices: MR imaging evaluation. *Radiology* **1988**;168:713–719
10. Teitelbaum GP, Raney M, Carvlin MJ, Matsumoto AH, Barth KH. Evaluation of ferromagnetism and magnetic resonance imaging artifacts of the Strecker tantalum vascular stent. *Cardiovasc Intervent Radiol* **1989**;12:125–127
11. Girard MT, Hahn PF, Saini S, Dawson SL, Goldberg MA, Mueller PR. Wallstent metallic biliary endoprosthesis: MR imaging characteristics. *Radiology* **1992**;184:874–876
12. Scott NA, Pettigrew RI. Absence of movement of coronary stents after placement in a magnetic resonance imaging field. *Am J Cardiol* **1994**;73:900–901
13. Tay HP, Juma S. Magnetic resonance imaging of the UroLume urethral stent. *J Urol* **1995**;153:1225–1226
14. Laissy JP, Grand C, Matos C, Struyven J, Berger JF, Schouman-Claeys E. Magnetic resonance angiography of intravascular endoprostheses: investigation of three devices. *Cardiovasc Intervent Radiol* **1995**;18:360–366
15. Taal BG, Muller SH, Boot H, Koops W. Potential risks and artifacts of magnetic resonance imaging of self-expandable esophageal stents. *Gastrointest Endosc* **1997**;46:424–429
16. Shellock FG, Kanal E. *Magnetic resonance: bioeffects, safety and patient management.* New York: Lippincott-Raven, **1996**
17. Shellock FG. *Pocket guide to metallic implants and MR procedures: update 1999.* New York: Lippincott-Raven, **1999**
18. Clerc CO, Jedwab MR, Mayer DW, Thompson PJ, Stinson JS. Assessment of ASTM F1058 cobalt alloy properties for permanent surgical implants. *J Biomed Mater Res* **1997**;38:229–234
19. American Society for Testing and Materials. Standard specification for the requirements and disclosure of self-closing aneurysm clips. In: *Annual book of ASTM standards.* West Conshohken, PA: American Society for Testing and Materials, **1994**
20. Shellock FG, Detrick MS, Brant-Zawadski M. MR-compatibility of Guglielmi detachable coils. *Radiology* **1997**;203:568–570
21. Shellock FG, Shellock VJ. Evaluation of cranial flap fixation clamps for compatibility with MR imging. *Radiology* **1998**;207:822–825
22. Shellock FG, Kanal E. Yasargil aneurysm clips: evaluation of interactions with a 1.5-Tesla MR system. *Radiology* **1998**;207:587–591
23. Kagetsu N, Litt A. Important considerations in measurement of attractive force on metallic implants in MR imagers. *Radiology* **1991**;179:505–508
24. Shellock FG. Compatibility of an endoscope designed for use in interventional MR imaging procedures. *AJR* **1998**;171:1297–1300
25. Chou C-K, McDougall JA, Chan KW. RF heating of implanted spinal fusion stimulator during magnetic resonance imaging. *IEEE Trans Biomed Eng* **1997**;44:357–373
26. Shellock FG, Shellock VJ. Vascular access ports and catheters tested for ferromagnetism, heating, and artifacts associated with MR imaging. *Magn Reson Imaging* **1996**;14:443–447
27. Shellock FG, Shellock VJ. Spetzler titanium aneurysm clips: compatibility of MR imaging. *Radiology* **1998**;206:838–841
28. Houdas Y, Ring EFJ. Temperature distribution. In: *Human body temperature: its measurements and distribution.* New York: Plenum, **1982**:68–84
29. National Council on Radiation Protection and Measurements (NCRP). Biological effects and exposure criteria for radiofrequency electromagnetic fields. Bethesda, MD: NCRP, **1986**. Report no. 86
30. Davis PL, Crooks L, Arakawa M, McRee R, Kaufman L, Margulis AR. Potential hazards in NMR imaging: heating effects of changing magnetic fields and RF fields on small metallic implants. *AJR* **1981**;137:857–860

This article has been cited by:

1. Ulrike Grzyska, Thomas Friedrich, Malte M. Sieren, Erik Stahlberg, Thekla H. Oechtering, Mandy Ahlborg, Thorsten M. Buzug, Alex Frydrychowicz, Joerg Barkhausen, Julian Haegele, Franz Wegner. 2021. Heating of an Aortic Stent for Coarctation Treatment During Magnetic Particle Imaging and Magnetic Resonance Imaging—A Comparative In Vitro Study. *CardioVascular and Interventional Radiology* **62**. . [Crossref]
2. Christian David Schenk, Rolf Gebker, Alexander Berger, Burkert Pieske, Christian Stehning, Sebastian Kelle. 2021. Review of safety reports of cardiac MR-imaging in patients with recently implanted coronary artery stents at various field strengths. *Expert Review of Medical Devices* **18**:1, 83-90. [Crossref]
3. Pejman Jabehdar Maralani, Nicola Schieda, Elizabeth M. Hecht, Harold Litt, Nicole Hindman, Chinthaka Heyn, Matthew S. Davenport, Greg Zaharchuk, Christopher P. Hess, Jeffrey Weinreb. 2020. MRI safety and devices: An update and expert consensus. *Journal of Magnetic Resonance Imaging* **51**:3, 657-674. [Crossref]
4. Franz Wegner, Thomas Friedrich, Nikolaos Panagiotopoulos, Sarah Valmaa, Jan P Goltz, Florian M Vogt, Martin A Koch, Thorsten M Buzug, Joerg Barkhausen, Julian Haegele. 2018. First heating measurements of endovascular stents in magnetic particle imaging. *Physics in Medicine & Biology* **63**:4, 045005. [Crossref]
5. Manuel Murbach, Earl Zastrow, Esra Neufeld, Eugenia Cabot, Wolfgang Kainz, Niels Kuster. 2015. Heating and Safety Concerns of the Radio-Frequency Field in MRI. *Current Radiology Reports* **3**:12. . [Crossref]
6. K. Müllerleile, C. Kolb, H. Rittger, K. Rybak, C. Tillmans, U. Wiegand, U. Sechtem, M. Kelm, J. Schulz-Menger. 2015. Passive kardiovaskuläre Implantate in der Magnetresonanztomographie. *Der Kardiologe* **9**:4, 303-309. [Crossref]
7. M Hasegawa, K Miyata, Y Abe, T Ishii, T Ishigami, K Ohtani, E Nagai, T Ohyama, Y Umekawa, S Nakabayashi. 2015. 3-T MRI safety assessments of magnetic dental attachments and castable magnetic alloys. *Dentomaxillofacial Radiology* **44**:6, 20150011. [Crossref]
8. Stanislav Vrtnik, Magdalena Wencka, Andreja Jelen, Hae Kim, Janez Dolinšek. 2015. Coronary stent as a tubular flow heater in magnetic resonance imaging. *Journal of Analytical Science and Technology* **6**:1, 1. [Crossref]
9. Hui-Zhe Li, Jian Xu. 2014. MRI compatible Nb–Ta–Zr alloys used for vascular stents: Optimization for mechanical properties. *Journal of the Mechanical Behavior of Biomedical Materials* **32**, 166-176. [Crossref]
10. F. Delgado, A. Saiz, A. Hilario, E. Murias, L. San Román Manzanera, A. Lagares Gomez-Abascal, A. Gabarrós, A. González García. 2014. Seguimiento mediante técnicas de neuroimagen de los aneurismas cerebrales tratados por vía endovascular. *Radiología* **56**:2, 118-128. [Crossref]
11. F. Delgado, A. Saiz, A. Hilario, E. Murias, L. San Román Manzanera, A. Lagares Gomez-Abascal, A. Gabarrós, A. González García. 2014. Neuroimaging follow-up of cerebral aneurysms treated with endovascular techniques. *Radiología (English Edition)* **56**:2, 118-128. [Crossref]
12. William P. Dillon, Christopher F. Dowd. Neurologic Complications of Imaging Procedures 1089-1105. [Crossref]
13. Govind Srinivasan, Joseph B. Selvanayagam. Emerging Role of Magnetic Resonance Imaging in the Evaluation of Coronary Atherosclerosis 177-185. [Crossref]
14. Jason W. Curtis, Donna C. Lesniak, James H. Wible, Pamela K. Woodard. 2013. Cardiac magnetic resonance imaging safety following percutaneous coronary intervention. *The International Journal of Cardiovascular Imaging* **29**:7, 1485-1490. [Crossref]
15. Frank G. Shellock, Cristen J. Giangarra. 2013. In vitro assessment of 3-T MRI issues for a bioabsorbable, coronary artery scaffold with metallic markers. *Magnetic Resonance Imaging* . [Crossref]
16. Nina Lopič, Andreja Jelen, Stanislav Vrtnik, Zvonko Jagličić, Magdalena Wencka, Radovan Starc, Aleš Blinc, Janez Dolinšek. 2013. Quantitative determination of magnetic force on a coronary stent in MRI. *Journal of Magnetic Resonance Imaging* **37**:2, 391-397. [Crossref]
17. Cihan Duran, Piotr S. Sobieszczyk, Frank J. Rybicki. Magnetic Resonance Imaging 166-183. [Crossref]
18. Davide Santoro, Lukas Winter, Alexander Müller, Julia Vogt, Wolfgang Renz, Celal Özerdem, Andreas Grässl, Valeriy Tkachenko, Jeanette Schulz-Menger, Thoralf Niendorf. 2012. Detailing Radio Frequency Heating Induced by Coronary Stents: A 7.0 Tesla Magnetic Resonance Study. *PLoS ONE* **7**:11, e49963. [Crossref]
19. Amedeo Chiribiri, Masaki Ishida, Eike Nagel, Rene M. Botnar. 2011. Coronary Imaging With Cardiovascular Magnetic Resonance: Current State of the Art. *Progress in Cardiovascular Diseases* **54**:3, 240-252. [Crossref]
20. Volker Rasche, Alexander Oberhuber, Stephan Trumpp, Axel Bornstedt, Karl-Heinz Orend, Nico Merkle, Wolfgang Rottbauer, Martin Hoffmann. 2011. MRI assessment of thoracic stent grafts after emergency implantation in multi trauma patients: a feasibility study. *European Radiology* **21**:7, 1397-1405. [Crossref]

21. W. G. Hundley, D. A. Bluemke, J. P. Finn, S. D. Flamm, M. A. Fogel, M. G. Friedrich, V. B. Ho, M. Jerosch-Herold, C. M. Kramer, W. J. Manning, M. Patel, G. M. Pohost, A. E. Stillman, R. D. White, P. K. Woodard. 2010. ACCF/ACR/AHA/NASCI/SCMR 2010 Expert Consensus Document on Cardiovascular Magnetic Resonance: A Report of the American College of Cardiology Foundation Task Force on Expert Consensus Documents. *Circulation* **121**:22, 2462-2508. [Crossref]
22. W. Gregory Hundley, David A. Bluemke, J. Paul Finn, Scott D. Flamm, Mark A. Fogel, Matthias G. Friedrich, Vincent B. Ho, Michael Jerosch-Herold, Christopher M. Kramer, Warren J. Manning, Manesh Patel, Gerald M. Pohost, Arthur E. Stillman, Richard D. White, Pamela K. Woodard. 2010. ACCF/ACR/AHA/NASCI/SCMR 2010 Expert Consensus Document on Cardiovascular Magnetic Resonance. *Journal of the American College of Cardiology* **55**:23, 2614-2662. [Crossref]
23. Rajesh Puranik, Vivek Muthurangu, David S. Celermajer, Andrew M. Taylor. 2010. Congenital Heart Disease and Multi-modality Imaging. *Heart, Lung and Circulation* **19**:3, 133-144. [Crossref]
24. Reza Nezafat, René M. Botnar, Kraig V. Kissinger, Peng Hu, Warren J. Manning. Coronary Artery and Vein Imaging 284-298. [Crossref]
25. Jérôme Jehl, Alexandre Comte, Sébastien Aubry, Nicolas Meneveau, François Schiele, Bruno Kastler. 2009. Clinical safety of cardiac magnetic resonance imaging at 3 T early after stent placement for acute myocardial infarction. *European Radiology* **19**:12, 2913-2918. [Crossref]
26. Julia Reinhardt, Thien-Hoa Nguyen-Trong, Stefan Hähnel, Matthias E. Bellemann, Sabine Heiland. 2009. Magnetresonanztomographie von Stents: Quantitative MR-Untersuchungen in vitro bei 3 Tesla. *Zeitschrift für Medizinische Physik* **19**:4, 278-287. [Crossref]
27. Eric Larose, Julie Côté, Josep Rodés-Cabau, Bernard Noël, Gerald Barbeau, Edith Bordeleau, Santiago Miró, Bernard Brochu, Robert Delarochellière, Olivier F. Bertrand. 2009. Contrast-enhanced cardiovascular magnetic resonance in the hyperacute phase of ST-elevation myocardial infarction. *The International Journal of Cardiovascular Imaging* **25**:5, 519-527. [Crossref]
28. Mehmet Gungor Kaya, Kaan Okyay, Huseyin Yazici, Nihat Sen, Yusuf Tavil, Sedat Turkoglu, Timur Timurkaynak, Murat Ozdemir, Mustafa Cemri, Ridvan Yalcin, Atiye Cengel. 2009. Long-term clinical effects of magnetic resonance imaging in patients with coronary artery stent implantation. *Coronary Artery Disease* **20**:2, 138-142. [Crossref]
29. Kenneth B. Baker, Michael D. Phillips. Deep Brain Stimulation Safety: MRI and Other Electromagnetic Interactions 453-472. [Crossref]
30. William P. Dillon, Christopher F. Dowd. Neurological Complications of Imaging Procedures 999-1013. [Crossref]
31. G. N. Levine, A. S. Gomes, A. E. Arai, D. A. Bluemke, S. D. Flamm, E. Kanal, W. J. Manning, E. T. Martin, J. M. Smith, N. Wilke, F. S. Shellock. 2007. Safety of Magnetic Resonance Imaging in Patients With Cardiovascular Devices: An American Heart Association Scientific Statement From the Committee on Diagnostic and Interventional Cardiac Catheterization, Council on Clinical Cardiology, and the Council on Cardiovascular Radiology and Intervention: Endorsed by the American College of Cardiology Foundation, the North American Society for Cardiac Imaging, and the Society for Cardiovascular Magnetic Resonance. *Circulation* **116**:24, 2878-2891. [Crossref]
32. Giuseppe D'Avenio, Rossella Canese, Franca Podo, Mauro Grigioni. 2007. A novel method for measuring the torque on implantable cardiovascular devices in MR static fields. *Journal of Magnetic Resonance Imaging* **26**:5, 1368-1374. [Crossref]
33. Warren J. Manning, Reza Nezafat, Evan Appelbaum, Peter G. Danias, Thomas H. Hauser, Susan B. Yeon. 2007. Coronary Magnetic Resonance Imaging. *Magnetic Resonance Imaging Clinics of North America* **15**:4, 609-637. [Crossref]
34. Edward T. Martin, David A. Sandler. 2007. MRI in patients with cardiac devices. *Current Cardiology Reports* **9**:1, 63-71. [Crossref]
35. Warren J. Manning, Reza Nezafat, Evan Appelbaum, Peter G. Danias, Thomas H. Hauser, Susan B. Yeon. 2007. Coronary Magnetic Resonance Imaging. *Cardiology Clinics* **25**:1, 141-170. [Crossref]
36. J. Kemper, A. N. Priest, D. Schulze, B. Kahl-Nieke, G. Adam, A. Klocke. 2007. Orthodontic springs and auxiliary appliances: assessment of magnetic field interactions associated with 1.5 T and 3 T magnetic resonance systems. *European Radiology* **17**:2, 533-540. [Crossref]
37. Robert Jan M. van Geuns, Timo Baks. Magnetic Resonance Imaging for Restenosis 277-285. [Crossref]
38. Paula Tejedor-Viñuela, José A. San Román-Calvar, Juan M. Durán-Hernández, Itziar Gómez-Salvador, José Sierra-Román, Francisco Fernández-Avilés. 2006. Seguridad de la realización precoz de un estudio de resonancia magnética cardiaca en pacientes con infarto agudo de miocardio y revascularización con stent. *Revista Española de Cardiología* **59**:12, 1261-1267. [Crossref]
39. Paula Tejedor-Viñuela, José A. San Román-Calvar, Juan M. Durán-Hernández, Itziar Gómez-Salvador, José Sierra-Román, Francisco Fernández-Avilés. 2006. Safety of Early Cardiac Magnetic Resonance Imaging in Acute Myocardial Infarction Patients With Stents. *Revista Española de Cardiología (English Edition)* **59**:12, 1261-1267. [Crossref]
40. Piotr Sobieszczyk, Martin J. Lipton, E. Kent Yucel. Magnetic Resonance Imaging 166-187. [Crossref]

41. Martin Busch, Wolfgang Vollmann, Thomas Bertsch, Rainer Wetzler, Axel Bornstedt, Bernhard Schnackenburg, Jörg Schnorr, Dietmar Kivelitz, Matthias Taupitz, Dietrich Grönemeyer. 2005. On the heating of inductively coupled resonators (stents) during MRI examinations. *Magnetic Resonance in Medicine* **54**:4, 775-782. [Crossref]
42. Evan Appelbaum, Ren?? M. Botnar, Susan B. Yeon, Warren J. Manning. 2005. Coronary magnetic resonance imaging: current state-of-the-art. *Coronary Artery Disease* **16**:6, 345-353. [Crossref]
43. A. N. Raval. 2005. Real-Time Magnetic Resonance Imaging-Guided Stenting of Aortic Coarctation With Commercially Available Catheter Devices in Swine. *Circulation* **112**:5, 699-706. [Crossref]
44. Bernd Müller-Bierl, Hansjörg Graf, Günter Steidle, Fritz Schick. 2004. Compensation of magnetic field distortions from paramagnetic instruments by added diamagnetic material: Measurements and numerical simulations. *Medical Physics* **32**:1, 76-84. [Crossref]
45. Juan R. Ayuso, Teresa M. de Caralt, Mario Pages, Vicente Riambau, Carmen Ayuso, Marcelo Sanchez, María I. Real, Xavier Montaña. 2004. MRA is useful as a follow-up technique after endovascular repair of aortic aneurysms with nitinol endoprostheses. *Journal of Magnetic Resonance Imaging* **20**:5, 803-810. [Crossref]
46. Michael M. H. Teng, Fong Tsai, Adrian Jy-Kang Liou, Jiing-Feng Lirng, Feng-Chi Chang, Chao-Bao Luo, Hui-Cheng Cheng. 2004. Three-Dimensional Contrast-Enhanced Magnetic Resonance Angiography of Carotid Artery after Stenting. *Journal of Neuroimaging* **14**:4, 336-341. [Crossref]
47. Frank G. Shellock, John V. Crues. 2004. MR Procedures: Biologic Effects, Safety, and Patient Care. *Radiology* **232**:3, 635-652. [Crossref]
48. Stefan C. Kr??mer, Alexander Wall, David Maintz, Rainald Bachmann, Harald Kugel, Walter Heindel. 2004. 3.0 Tesla Magnetic Resonance Angiography of Endovascular Aortic Stent Grafts. *Investigative Radiology* **39**:7, 413-417. [Crossref]
49. Laurent Létourneau-Guillon, Gilles Soulez, Gilles Beaudoin, Vincent L. Oliva, Marie-France Giroux, Zhao Qin, Nicolas Boussion, Éric Therasse, Jacques de Guise, Guy Cloutier. 2004. CT and MR Imaging of Nitinol Stents with Radiopaque Distal Markers. *Journal of Vascular and Interventional Radiology* **15**:6, 615-624. [Crossref]
50. A. Kangarlu, K. T. Baudendistel, J. T. Heverhagen, M. V. Knopp. 2004. Klinische Hoch- und Ultrahochfeld-MR und ihre Wechselwirkung mit biologischen Systemen. *Der Radiologe* **44**:1, 19-30. [Crossref]
51. L W Bartels, C J G Bakker. 2003. Endovascular interventional magnetic resonance imaging. *Physics in Medicine and Biology* **48**:14, R37-R64. [Crossref]
52. JOLANDA J. WENTZEL, SILVIA H. AGUIAR, ZAHI A. FAYAD. 2003. Vascular MRI in the Diagnosis and Therapy of the High Risk Atherosclerotic Plaque. *Journal of Interventional Cardiology* **16**:2, 129-142. [Crossref]
53. Ryan J. Uitti, Yoshio Tsuboi, Robert A. Pooley, John D. Putzke, Margaret F. Turk, Zbigniew K. Wszolek, Robert J. Witte, Robert E. Wharen. 2002. Magnetic Resonance Imaging and Deep Brain Stimulation. *Neurosurgery* **51**:6, 1423-1431. [Crossref]
54. Frank G. Shellock. 2002. Biomedical implants and devices: Assessment of magnetic field interactions with a 3.0-Tesla MR system. *Journal of Magnetic Resonance Imaging* **16**:6, 721-732. [Crossref]
55. Ryan J. Uitti, Yoshio Tsuboi, Robert A. Pooley, John D. Putzke, Margaret F. Turk, Zbigniew K. Wszolek, Robert J. Witte, Robert E. Wharen. 2002. Magnetic Resonance Imaging and Deep Brain Stimulation. *Neurosurgery* **51**:6, 1423-1431. [Crossref]
56. Ron C. Gaba, Ruth C. Carlos, William J. Weadock, Gautham P. Reddy, Michael B. Sneider, Philip N. Cascade. 2002. Cardiovascular MR Imaging: Technique Optimization and Detection of Disease in Clinical Practice. *RadioGraphics* **22**:6, e6-e6. [Crossref]
57. Frank G. Shellock. 2002. Magnetic resonance safety update 2002: Implants and devices. *Journal of Magnetic Resonance Imaging* **16**:5, 485-496. [Crossref]
58. Siegfried Thurnher, Manfred Cejna. 2002. Imaging of aortic stent-grafts and endoleaks. *Radiologic Clinics of North America* **40**:4, 799-833. [Crossref]
59. Wilson Greatbatch, Victor Miller, Frank G. Shellock. 2002. Magnetic resonance safety testing of a newly-developed fiber-optic cardiac pacing lead. *Journal of Magnetic Resonance Imaging* **16**:1, 97-103. [Crossref]
60. Elmar M. Merkle, Stefan Klein, Christian Wisianowsky, Daniel T. Boll, Thorsten R. Fleiter, Reinhard Pamler, Johannes Görich, Hans-Jürgen Brambs. 2002. Magnetic Resonance Imaging Versus Multislice Computed Tomography of Thoracic Aortic Endografts. *Journal of Endovascular Therapy* **9**:SupplementII, II-2-II-13. [Crossref]
61. Elmar M. Merkle, Stefan Klein, Christian Wisianowsky, Daniel T. Boll, Thorsten R. Fleiter, Reinhard Pamler, Johannes Görich, Hans-Jürgen Brambs. 2002. Magnetic Resonance Imaging versus Multislice Computed Tomography of Thoracic Aortic Endografts. *Journal of Endovascular Therapy* **9**:2_suppl, II-2-II-13. [Crossref]

62. Elmar M. Merkle, Stefan Klein, Stefan C. Krämer, Christian Wisianowsky. 2002. MR Angiographic Findings in Patients with Aortic Endoprostheses. *American Journal of Roentgenology* **178**:3, 641-648. [Citation] [Full Text] [PDF] [PDF Plus]
63. Ali R. Rezai, Daniel Finelli, John A. Nyenhuis, Greg Hrdlicka, Jean Tkach, Ashwini Sharan, Paul Rugieri, Paul H. Stypulkowski, Frank G. Shellock. 2002. Neurostimulation systems for deep brain stimulation: In vitro evaluation of magnetic resonance imaging-related heating at 1.5 tesla. *Journal of Magnetic Resonance Imaging* **15**:3, 241-250. [Crossref]
64. Lambertus W. Bartels, Chris J.G. Bakker, Max A. Viergever. 2002. Improved lumen visualization in metallic vascular implants by reducing RF artifacts. *Magnetic Resonance in Medicine* **47**:1, 171-180. [Crossref]
65. André J. Duerinckx. The Coronary Arteries 257-282. [Crossref]
66. DIETMAR KIVELITZ, SUSANNE WAGNER, JÖRG HANSEL, JÖRG SCHNORR, RAINER WETZLER, MARTIN BUSCH, ANDREAS MELZER, MATTHIAS TAUPITZ, BERND HAMM. 2001. The Active Magnetic Resonance Imaging Stent (AMRIS). *Investigative Radiology* **36**:11, 625-631. [Crossref]
67. Frank G. Shellock. 2001. Metallic neurosurgical implants: Evaluation of magnetic field interactions, heating, and artifacts at 1.5-Tesla. *Journal of Magnetic Resonance Imaging* **14**:3, 295-299. [Crossref]
68. Elmar M. Merkle, Daniel T. Boll, Hans Weidenbach, Hans-Jürgen Brambs, Andreas Gabelmann. 2001. Ability of MR Cholangiography to Reveal Stent Position and Luminal Diameter in Patients with Biliary Endoprostheses. *American Journal of Roentgenology* **176**:4, 913-918. [Abstract] [Full Text] [PDF] [PDF Plus]
69. Sven Adamsen, Søren Meisner. 2001. Expandable metal stents for malignant colorectal obstruction. *Techniques in Gastrointestinal Endoscopy* **3**:2, 103-107. [Crossref]
70. DAVID MAINTZ, HARALD KUGEL, FRANK SCHELLHAMMER, AND PETER LANDWEHR. 2001. In Vitro Evaluation of Intravascular Stent Artifacts in Three-Dimensional MR Angiography. *Investigative Radiology* **36**:4, 218-224. [Crossref]
71. Frank G. Shellock. 2001. Metallic surgical instruments for interventional MRI procedures: Evaluation of MR safety. *Journal of Magnetic Resonance Imaging* **13**:1, 152-157. [Crossref]
72. Anne M. Sawyer-Glover, Frank G. Shellock. 2000. Pre-MRI procedure screening: recommendations and safety considerations for biomedical implants and devices. *Journal of Magnetic Resonance Imaging* **12**:3, 510-510. [Crossref]
73. Maria-Benedicta Edwards, Kenneth M. Taylor, Frank G. Shellock. 2000. Prosthetic heart valves: Evaluation of magnetic field interactions, heating, and artifacts at 1.5 T. *Journal of Magnetic Resonance Imaging* **12**:2, 363-369. [Crossref]
74. Frank G. Shellock. 2000. Radiofrequency Energy-Induced Heating During MR Procedures: A Review. *Journal of Magnetic Resonance Imaging* **12**:1, 30-36. [Crossref]
75. Allahyar Kangarlu, Frank G. Shellock. 2000. Aneurysm Clips: Evaluation of Magnetic Field Interactions With an 8.0 T MR System. *Journal of Magnetic Resonance Imaging* **12**:1, 107-111. [Crossref]
76. Anne M. Sawyer-Glover, Frank G. Shellock. 2000. Pre-MRI Procedure Screening: Recommendations and Safety Considerations for Biomedical Implants and Devices. *Journal of Magnetic Resonance Imaging* **12**:1, 92-106. [Crossref]
77. Allahyar Kangarlu, Frank G. Shellock. 2000. Aneurysm Clips: Evaluation of Magnetic Field Interactions With an 8.0 T MR System. *Journal of Magnetic Resonance Imaging* **12**:1, 107-111. [Crossref]
78. CHRISTOPH MANKE, WOLFGANG R. NITZ, MARKUS LENHART, MARKUS VÖLK, ANGELA GEISSLER, STEFAN FEUERBACH, JOHANN LINK. 2000. Magnetic Resonance Monitoring of Stent Deployment. *Investigative Radiology* **35**:6, 343-351. [Crossref]
79. Allahyar Kangarlu, Pierre-Marie L. Robitaille. 2000. Biological effects and health implications in magnetic resonance imaging. *Concepts in Magnetic Resonance* **12**:5, 321-359. [Crossref]
80. Allahyar Kangarlu, Pierre-Marie L. Robitaille. 2000. Biological effects and health implications in magnetic resonance imaging. *Concepts in Magnetic Resonance* **12**:5, 321-359. [Crossref]
81. Vivek Muthurangu, Reza Razavi, Jan Bogaert, Andrew M. Taylor. Congenital Heart Disease 439-473. [Crossref]
82. Reza Razavi, Vivek Muthurangu, Sanjeet R. Hegde, Andrew M. Taylor. MR-Guided Cardiac Catheterization 513-538. [Crossref]
83. Virna Zampa, Marzio Perri, Simona Ortori. Abdominal aorta 357-375. [Crossref]
84. Andé J. Duerinckx. Clinical Applications Today 68-81. [Crossref]